

Invited Contribution from Recipient of ACS Award for Distinguished Service in the Advancement of Inorganic Chemistry

Exploratory Synthesis in the Solid State. Endless Wonders[†]

John D. Corbett

Department of Chemistry and Ames Laboratory, Iowa State University, Ames, Iowa 50011

Received July 14, 2000

It is always difficult to predict the unimaginable

This article gives an overview of recent developments in three areas of solid state chemistry: (1) The discovery that centered and originally-adventitious interstitial elements Z are essential for the stability of M_6X_{12} -type cluster halides of group 3 and 4 metals has led to a large amount of new chemistry through tuning structures and compositions of $A_nM_6(Z)X_{12}X_n$ phases with the variables Z, x, and n. The corresponding metal-rich group 3 tellurides exhibit novel and more extensive metal aggregation, reflecting a decreased number of anions and valence electrons. (2) Many intrinsically metallic T_5M_3 phases with a Mn_5Si_3 -type structure are formed by early transition metals T with main-group elements M. Each characteristically reacts with diverse elements (up to 15–20 each) to form stuffed interstitial versions T_5M_3Z of the same structure. The ranges of Z and some properties are described. Related reactions of hydrogen (often as an impurity) in Mn_5Si_3 -, β - Yb_5Sb_3 -, and Cr_5B_3 -type systems are extensive. Substantially all previous reports of β - Yb_5Sb_3 - and Cr_5B_3 -type phases for divalent metals with pnictogen (As–Bi) and tetrel (Si–Pb) elements, respectively, have been for the hydrides, and about two-thirds do not exist without that hydrogen (or fluorine). (3) The developing chemistry of anionic polymetal cluster compounds of the main-group elements with alkali-metal cations is outlined, particularly for the triel elements In and Tl. These clusters lie to the left of what has been called the Zintl boundary, many are new hypoelectronic polyhedra, some may be centered by the same or another neighboring element, and so far all have been isolated only as neat solid state compounds in which specificity of cation–anion interactions seems important. Extended networks are also encountered.

Introduction

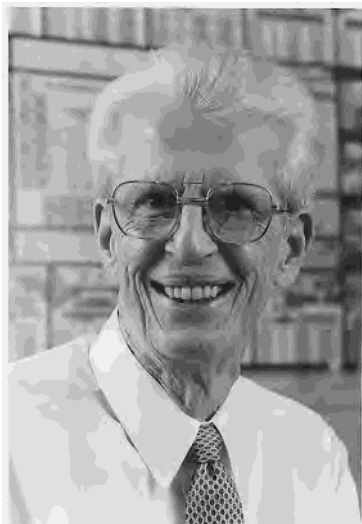
Since this Award follows on my 1986 ACS Award in Inorganic Chemistry, I will concentrate in this article on the revelations and accomplishments in the 15 years since the earlier nomination. Happily, these turn out to be quite distinctive, although they still follow on the general theme of exploratory synthesis, structure, and properties in solid state chemistry, particularly as they pertain to new chemistry along the interface between metals and salts.

[†] This article is based on the address for the 2000 ACS Award for Distinguished Service in the Advancement of Inorganic Chemistry that was presented as INOR 324 at the 219th National Meeting of the American Chemical Society, San Francisco, CA, March 27, 2000.

The following general observations anticipate the subsequent details:

1. Clusters and their networks are common.
2. The salt–metal differentiation is shrinking.
3. Numerous structures are dominated by robust metal–metal bonding: 1-, 2-, 3-D.
4. Electron counting regularities are not always applicable to solids.
5. There is chemistry *in* intermetallics.
6. There is *much* to be discovered that cannot be imagined.

It is the wonder and excitement of finding the unprecedented and unimaginable that makes the research enjoyable, even exhilarating, and worthwhile.



John D. Corbett was born in Yakima, WA, in 1926. After service in V-12 units in the midwest during World War II, he went on to finish his B.S. (1948) and Ph.D. (1952) degrees at the University of Washington, the latter with Norman W. Gregory in physical chemistry. He has been associated with the Department of Chemistry and Ames Laboratory (DOE) at Iowa State University ever since, where he is presently Professor of Chemistry, Distinguished Professor in the College of Liberal Arts and Sciences, and Senior Chemist. The general long-term focus of his program has been wide-ranging exploratory synthesis along metal–salt interfaces coupled with structural and bonding characterizations. Corbett earlier received the 1986 ACS Award in Inorganic Chemistry, an Alexander von Humboldt Senior Scientist Award, and two Department of Energy Awards in Materials Chemistry. He is a member of the National Academy of Sciences. (Photograph reprinted with permission from Corbett, J. D. *Angew. Chem., Int. Ed.* **2000**, 39, 670. Copyright 2000 Wiley-VCH.)

The discoveries will be covered in three relatively distinct areas, as follows: (1) Cluster halides of the early transition metals that *require* interstitial heteroatoms, and recently discovered telluride analogues (review¹). (2) A broad family of transition-metal–intermetallic phases with Mn_5Si_3 -type structures that show extensive interstitial chemistries,² and some related instances of hydride impurity effects. (3) Polyatomic cluster anions and networks of the main-group metals, their bonding rules, and Zintl phases.³ All of these experimentally utilize generally similar reaction and characterization techniques, especially more-or-less high temperature (300–1400 °C) reactions contained in welded tantalum or niobium tubing, glovebox manipulations, and Guinier X-ray powder diffraction as a sensitive means of phase detection and lattice parameter determination. Many of the products are quite air-sensitive, but the remainder of the methods and techniques employed are fairly routine in solid state chemistry.

I. Interstitially-Stabilized Cluster Halides

The first basic secrets of this puzzling area had just been recognized 15 years ago: that once-adventitious impurities as centered interstitials in Zr_6Cl_{12} , Sc_6Cl_{12} , and other clusters as well as in layered lanthanide monohalides⁴ were responsible for the appearance of relatively small amounts of unusual phases and other features. (The term “garbage chemistry” was once aptly applied.⁵) Carbon is in everyone’s glovebox in some form,

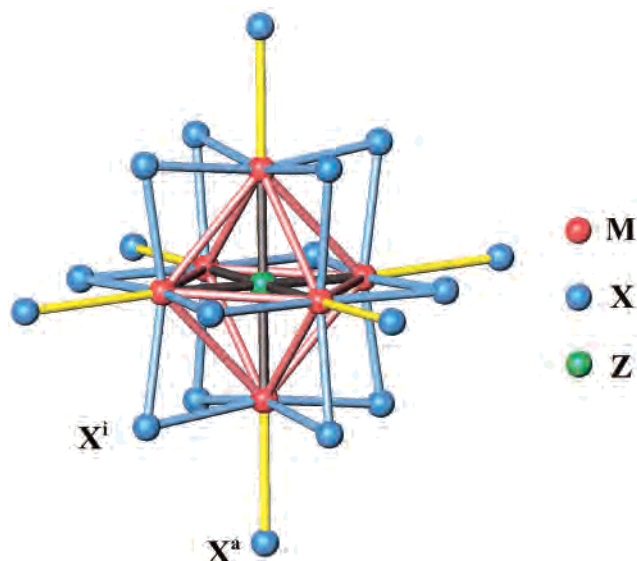


Figure 1. The basic octahedral cluster halide $R_6(Z)(X^i)_{12}(X^a)_6$ for group 3 or 4 metals and $X = Cl, Br, \text{ or } I$ (blue). All clusters contain an interstitial Z (green) atom.

and just a few well-formed crystals can evince surprisingly small amounts of this or other common elements, especially in the presence of a gemisch of uninteresting microcrystalline products ($ZrCl_3$, $ZrCl_2$, Zr , etc.). The earliest clarifications were achieved through directed high-yield syntheses and structural characterizations of, for example, $Sc_7Cl_{10}C_2$,⁶ $Zr_6Cl_{14}C$, $KZr_6Cl_{13}Be$,⁷ $Zr_6I_{12}C$,⁸ Zr_2Cl_2N ,⁹ and $Sc_7I_{12}C^{10}$ in which an atom of the last-listed nonmetal was found to be centered in each nominally octahedral metal cluster. These revelations were accompanied by the additional general realization that all of the reported double-metal-layered rare-earth-metal (R) monohalides RX ($X = Cl, Br, I$ throughout) and their derivatives were actually ternary or higher hydrides.^{11,12} The subsequent Edisonian exploration of appreciable portions of the period table for potential interstitials has revealed not only how widely distributed this new chemistry is but also the versatility and very large structural variety that interstitials and other features allow, and the useful valence rules that pertain.

Discrete Clusters. The extensive range of structures and compositions all derive from the basic building block shown in Figure 1, a metal octahedron $M_6(Z)X_{12}$ with all 12 edges of M_6 bridged by halide (blue) and centered by some heteroatom Z (green). The electronic requirements for the metal framework encapsulating a main-group interstitial consist of, in decreasing binding energy, a_{1g}^2 , t_{1u}^6 , t_{2g}^6 , which lead to an optimal 14 skeletal electrons for a closed-shell cluster.^{8,13} In general, the a_{2u} LUMO lies fairly high for a relatively undistorted cluster (i.e., one in which the metal vertices fall near the faces of a cube defined by halogen atoms on all edges), although this energy level will fall in the presence of substantial matrix effects

(5) McCarley, R. E., personal communication, Cedar Rapids, IA, 1984.

(6) Hwu, S.-J.; Corbett, J. D.; Poeppelmeier, K. R. *J. Solid State Chem.* **1985**, 57, 43.

(7) Ziebarth, R. P.; Corbett, J. D. *J. Am. Chem. Soc.* **1985**, 107, 4571.

(8) Smith, J. D.; Corbett, J. D. *J. Am. Chem. Soc.* **1985**, 107, 5704.

(9) Hwu, S.-J.; Ziebarth, R. P.; von Winbush, S.; Ford, J. E.; Corbett, J. D. *Inorg. Chem.* **1986**, 25, 283.

(10) Dudis, D. S.; Corbett, J. D.; Hwu, S.-J. *Inorg. Chem.* **1986**, 25, 3434.

(11) Mattausch, H.; Schramm, W.; Eger, R.; Simon, A. *Z. Anorg. Allg. Chem.* **1985**, 530, 43.

(12) Meyer, G.; Hwu, S.-J.; Wijeyesekera, S.; Corbett, J. D. *Inorg. Chem.* **1986**, 25, 4811.

(13) Smith, J. D.; Corbett, J. D. *J. Am. Chem. Soc.* **1986**, 108, 1927.

(1) Corbett, J. D. *J. Alloys Compd.* **1995**, 229, 10.

(2) Corbett, J. D.; Garcia, E.; Guloy, A. M.; Hurng, W.-M.; Kwon, Y.-U.; Leon-Escamilla, E. A. *Chem. Mater.* **1999**, 10, 2824.

(3) Corbett, J. D. *Angew. Chem., Int. Ed.* **2000**, 39, 670.

(4) Simon, A. *J. Solid State Chem.* **1985**, 57, 2.

(crowding) that put the metal vertices inside the cube faces. This means a 16-electron limit will become more important with the smaller Nb₆X₁₂ or Ta₆X₁₂ units, or when a larger halide is coupled with a particularly small interstitial (e.g., Zr₆I₁₂C, 6 × 4 + 4 – 12 × 1 = 16 electrons).¹⁴ Encapsulation of a transition element with d orbitals adds an additional nonbonding e_g⁴ level that is centered largely only on Z, while the added t_{2g} and the former t_{1u} exchange former roles in cluster vs framework bonding.^{15,16} (The p orbitals on transition metal Z are generally too high lying to be important.) The optimal count is then 18, as in Zr₆I₁₄Fe, giving rise to the amusing result that C and Fe atoms with 4 and 8 valence electrons are sort of isoelectronic in their effects in closed-shell cluster bonding in, say, Zr₆Cl₁₄C (14e) vs Zr₆Cl₁₄Fe (18e).

Encapsulation of interstitials with diverse valence electron counts is the first step to gaining a large variety of cluster phases. The second comes from varied halide functionalities possible about the clusters. The discrete 6–12–6-type cluster shown in Figure 1 has, in addition to the nearly inevitable 12 inner edging-bridging members Xⁱ, six more X^a that are strongly bonded exo or terminal at cluster vertices (which otherwise would be highly reactive, an empty hemisphere about a cluster metal with d valence orbitals). There can be some variety in the functionality of the last six halides, which may be (a) solely terminal X^a (a = outer (äusser)), (b) bridging between cluster vertices X^{a-a}, or (c) edge-bridging in one cluster and terminal in another, X^{i-a} and X^{a-i}. The last two modes generate networks of course. Even more condensed versions are also found, utilizing Xⁱ⁻ⁱ and X^{i-a-a} for example in more hypostoichiometric (X:M < 12:6) compounds, the degree of reduction of a M₆X cluster naturally varying inversely with the number of halides present. (Further reduction with cluster condensation will be noted later.) A third tuning opportunity exists through insertion (intercalation) of alkali-metal (or other) cations into the cavities in the cluster structure that are defined by halogen. Their addition reduces the cluster, either directly as added alkali metal or through countering the oxidation produced by added halide. Thus we come to a general formulation of these cluster systems as



in which *x*, *Z*, and *n* are variables. Experimentally, examples are known for 0 ≤ *x*, *n* ≤ 6 without including examples with negative values for *n* (below). Thus, most of the questions regarding possible variety and range of new phases reduce to that of the existence of suitable three-dimensional structural motifs. The last is certainly not a significant limitation; the variety found well exceeds one's ability to conceive of the possibilities.¹⁷

A few isoelectronic sequences emphasize how these multiple variables can operate. With varying *x* and *Z*, Zr₆Cl₁₅N, KZr₆Cl₁₅C, K₂Zr₆Cl₁₅B, and K₃Zr₆Cl₁₅Be are all known and, for changing *x* and *n*, so are Zr₆Cl₁₃B, RbZr₆Cl₁₄B, Rb₂Zr₆Cl₁₅B, R₃Zr₆Cl₁₆B, and Rb₅Zr₆Cl₁₈B.¹⁸ The variety of *Z* possible for the workable group 4 and 3 (rare-earth) cluster metals are emphasized in Table 1 just for ternary systems. (Examples with

Table 1. Interstitial and Structural Variations among M₆X₁₂Z-Type Clusters

| cluster type | Z | | | | | structure M–X stoichiometries |
|-----------------------------------------------|----|----|----|----|---------------------------|-----------------------------------------------------------------|
| | Mn | Fe | Co | Ni | | |
| Zr ₆ Cl ₁₂ Z | | | | | H Be B C N | 6–12 + <i>n</i> , 0 ≤ <i>n</i> ≤ 6 ^a |
| Zr ₆ I ₁₂ Z | | | | | Be B C N Al Si P Ge | 6–14 6–12 |
| R ₆ I ₁₂ Z ^b | Cr | Mn | Fe | Co | B C (C ₂) | 7–12 6–14 ^a 6–13 ^a 6–10 6–8.5 |
| | | Mn | Fe | Co | Ni Cu | |
| | | | | | Ru Rh Pd | |
| | | | | | Re Os Ir Pt Au | |

^a The higher halide contents occur in quaternary phases with alkali metals. ^b R = rare-earth element.

Ti and Hf are few.) The categories of M:X proportions in known structure types are seen to be fairly different for (a) zirconium chlorides with 0 ≤ *n* ≤ 6, (b) zirconium iodides, where electron counts are not as restricted by “rules”, but M:X stoichiometries are seemingly limited to only two structure types in ternaries (6–12 and 6–14), and (c) clusters of the electron-poorer rare-earth metals which are generally more reduced, and where the variety of workable transition metals as *Z* really blossoms. It should be noted that the missing elements around the borders of these *Z* summaries usually signify that the incorporation was tried but that some collection of other products was instead more stable. (Our conditions inevitably yield equilibrium systems.) Thus the known, centered cluster halide compounds span over 40 structure types and several hundred compositions.

The structural and bonding principles have been considered elsewhere in some detail, including effective interstitial radii, more complex structures and compositions, matrix effects, and cation site problems.^{1,17} The last may be of relatively low symmetry, with the cavities (and the resultant cation ellipsoids) quite distorted, the cation interactions with neighboring halides often seeming to represent only a small fraction of the binding forces for the whole structure.

There is only time to illustrate a few of the ternary varieties M₆(Z)X_{12+n}. Figure 2 illustrates the beauty of one of the structures adopted by [Zr₆(Z)Clⁱ]₁₂(Cl^a)_{6/2} (*n* = 3) phases, showing how the Zr₆(Co) cores (the 12 Clⁱ about each are omitted from the figure for clarity) are interconnected into a cubic array by six bridging chlorides Cl^{a-a}.¹⁹ A remarkable feature of the structure is that two such equivalent lattices interpenetrate, without interconnection, one shown with orange Zr₆ clusters, yellow Co, and red Cl bridges and a second, with green clusters, purple Co, and blue Cl bridges. In this instance, the Co interstitial yields 18-electron clusters (6 × 4 + 9 – 15 × 1). A frequent method to force or tune a synthesis is to provide different components, and here Fe or Mn together with Li yields an isoelectronic and nominally isostructural phase LiZr₆(Fe)Cl₁₅ or Li₂Zr₆(Mn)Cl₁₅. There is room for only these small cations among the Clⁱ and Cl^a atoms, and bromide seems too large to allow this novel interpenetrating structure. Although there is potentially space for a third increment of Li, this does not yield yet another example with Cr, other products simply being more stable. A single example of this type was previously known for Nb₆F₁₅,²⁰ with no opportunity to couple interstitial encapsulation with cation insertion. There are five other

(14) Ziebarth, R. P.; Corbett, J. D. *J. Am. Chem. Soc.* **1989**, *111*, 3272.

(15) Hughbanks, T.; Rosenthal, G.; Corbett, J. D. *J. Am. Chem. Soc.* **1986**, *108*, 8289.

(16) Hughbanks, T.; Rosenthal, G.; Corbett, J. D. *J. Am. Chem. Soc.* **1988**, *110*, 1511.

(17) Corbett, J. D. *Modern Perspectives in Inorganic Crystal Chemistry*; NATO ASI; Parthé, E., Ed.; Kluwer Acad. Publ.: Dordrecht, Holland, 1992; p 27.

(18) Ziebarth, R. P.; Corbett, J. D. *Acc. Chem. Res.* **1989**, *22*, 256.

(19) Zhang, J.; Corbett, J. D. *Inorg. Chem.* **1991**, *30*, 431.

(20) Schäfer, H.; Schnering, H.-G.; Niehues, K.-J.; Nieder-Vahrenholz, H. *G. J. Less-Common Met.* **1965**, *9*, 95.

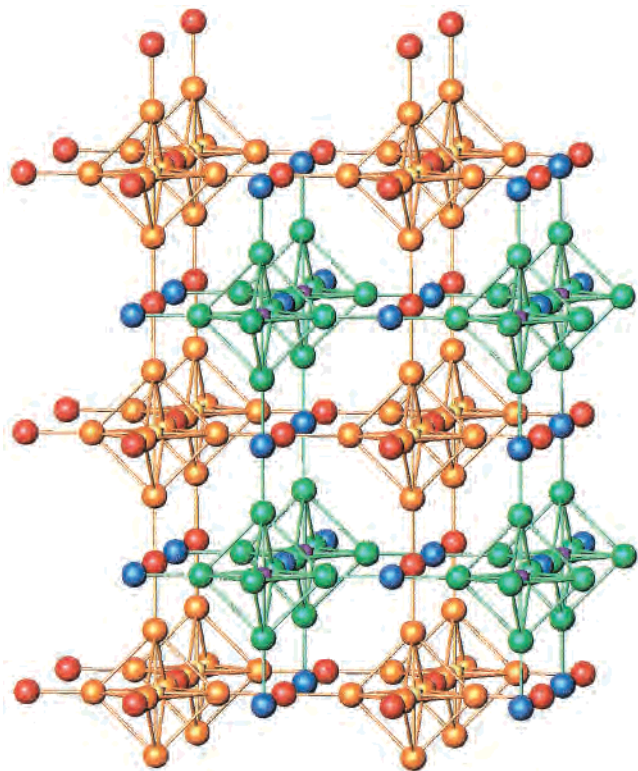


Figure 2. The cubic structure of $Zr_6(Co)(Cl)_{12}(Cl^{a-a})_{6/2}$ with all Clⁱ omitted for clarity. Note the two identical interpenetrating cluster networks: orange Zr_6 with yellow Co and red bridging Cl^{a-a} plus green Zr_6 , purple Co, and blue Cl^{a-a} .

connectivities by which $Zr_6(Z)X_{12}X_{6/2}$ compositions can be interlinked, and no interconversions can take place among these without bond breakage. Most of the compounds in this group include alkali-metal cations as well, and their sizes are usually critical.^{21,22}

Another structure, Figure 3, illustrates how the rare-earth element clusters achieve lower proportions of halogen, here in the formally hypostoichiometric $Pr_6(Ru)Br_{10}$.^{23–25} The complete functional description of the bromide about one cluster is $Pr_6(Ru)(Br^{i-i})_{4/2}(Br^{i-a})_2(Br^{i-a})_{6/2}(Br^{a-i})_{6/2}$. (Note (a) the conservation of Br^i (12), Br^a (6), and Br/Pr_6 (10) and (b) the stability of the network with three different Br basicities.) Pairs of the novel $i-i$ bridges in chains can be seen in Figure 3 (lighter blue) in the more nearly horizontal intercluster connections where they are paralleled by two Br^{i-a} bridges. The parallel $Br^{i-a}-Br^{a-i}$ functions that lie vertical are rather common and in this structure interbridge each cluster to others in the four remaining directions. It will be noted that this particular member of a rather compact structure type is achieved with only 16 cluster-based electrons. The t_{1u}^4 result in the HOMO (for the cubic representation) leads to a substantial Jahn–Teller compression in each cluster, the vertical $d(Pr-Ru)$ in this view being 0.28 Å (9.8%) shorter relative to the waist $Pr-Ru$ distances. The Os but not the Fe analogue is also known, as are 17- and 18-electron examples with later Z, some as iodides.

We will not be able to illustrate other important binary structure types, but these include $Zr_6X_{14}Z$,⁸ where a 2:1 combination of X^{a-a} and $X^{i-a}-X^{a-i}$ occupy exo positions and

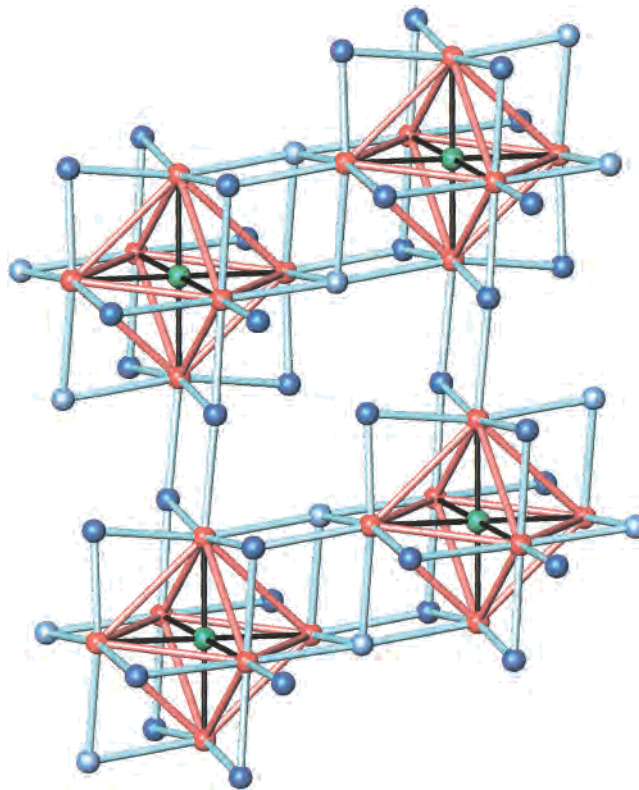


Figure 3. A [101] section of the repeating units in monoclinic $Pr_6(Ru)Br_{10}$. The novel Br^{i-i} bridging functions that enable this low Br:Pr proportion are lighter blue.

link the clusters, $Zr_6X_{12}Z$ where half of the X^i interbridge clusters as X^{i-a} ,^{26,27} and the unusual $Zr_6Cl_{13}B^7$ and $Zr_6Cl_{11.5}I_{1.5}B^{28}$ with Cl^{i-i} connections as well as a rare Cl^{a-a-a} connection. Further increases in chlorine content beyond 6:15 generate increasingly open structures, eventually without any interbridging between clusters for $Zr_6(Z)Cl_{18}^{x-}$ compositions, and all of these contain alkali-metal analogues do not seem nearly as prolific.

The generally halogen-poorer R_6X_{12} -type clusters built from the group 3 (rare-earth) elements share *no* common structure types with the group 4 (Zr) examples, Table 1. However, the rhombohedral $Zr_6X_{12}Z$ members just noted may be conceptually converted to a $(R^{3+})(R_6X_{12}Z)^{3-}$ derivative with the addition of a seventh metal as R^{3+} in a suitable cavity. Alkali-metal derivatives of this type are now also known, such as $NaSc_6(Os)I_{12}$ and $LiLa_6(Pt)I_{12}$.²⁹ Even the very reduced $Pr_{12}Fe_2I_{17}$ and others^{30,31} contain only separate 6–12-Fe-type clusters, wherein each cluster utilizes *seven* I^{i-i} interconnections to achieve the average stoichiometry $R_6(Z)I_{8.5}$.

Condensed Clusters. Undiscovered phases of course have unknown compositions, and so it is prudent to ensure that reaction stoichiometries range widely, not letting the latter be guided too much by prejudice and what is already known. Excess metal reactions have provided very novel condensed cluster phases. With zirconium, only the long-known, metallic $ZrCl$ and $ZrBr$ and some interstitial derivatives⁹ are found, the backbone in these being strongly-bonded double-metal layers

(21) Qi, R.-Y.; Corbett, J. D. *Inorg. Chem.* **1995**, *34*, 1646.

(22) Zhang, J.; Corbett, J. D. *Inorg. Chem.* **1995**, *34*, 1652.

(23) Hughbanks, T.; Corbett, J. D. *Inorg. Chem.* **1989**, *28*, 631.

(24) Payne, M. W.; Corbett, J. D. *Inorg. Chem.* **1990**, *29*, 2246.

(25) Llusar, R.; Corbett, J. D. *Inorg. Chem.* **1994**, *33*, 849.

(26) Hwu, S.-J.; Corbett, J. D. *J. Solid State Chem.* **1986**, *64*, 331.

(27) Hughbanks, T.; Corbett, J. D. *Inorg. Chem.* **1988**, *27*, 2022.

(28) Köckerling, M.; Qi, R.-Y.; Corbett, J. D. *Inorg. Chem.* **1996**, *35*, 1437.

(29) Uma, S.; Jensen, E.; Corbett, J. D. Unpublished research.

(30) Park, Y.; Corbett, J. D. *Inorg. Chem.* **1994**, *33*, 1705, 3848.

(31) Lulei, M.; Martin, J. D.; Corbett, J. D. *J. Solid State Chem.* **1996**, *125*, 249.

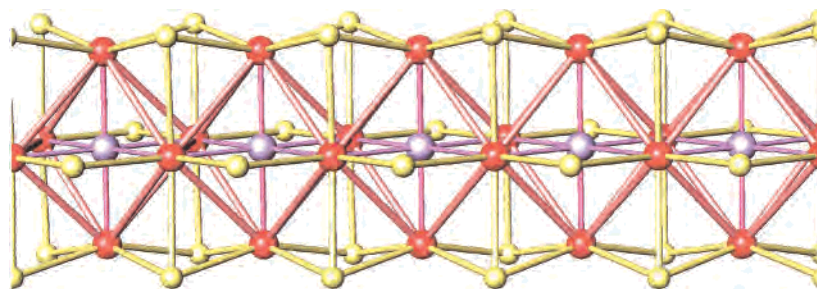


Figure 4. A segment of the infinite chain of trans-edge-sharing octahedra in $\text{Pr}_4(\text{Ru})\text{I}_5$. Halogen (yellow) from other chains completes the exo bonding about the chain. The red Ru–Pr bonds normal to the chain direction are distinctly shorter owing to $d\pi$ – $d\pi$ bonding.

sandwiched between double-halogen layers. The trivalent elements are, on the other hand, quite rich in condensed cluster products, particularly those structured from metal octahedra that share *trans*-metal edges to form chains, while only a few dimeric ($\text{Cs}_2\text{La}_{10}\text{I}_{17}\text{Ru}_2$ ³²) and tetrameric (such as $\text{Y}_{16}\text{Ir}_4\text{Br}_{36}$) oligomers^{33–35} have been found. A segment of one of the simpler chain structures is shown in Figure 4, $\text{Pr}_4\text{I}_5\text{Ru}$, in which $[\text{Pr}_2\text{Pr}_{4/2}(\text{Ru})]$ octahedral chains (red and lavender) are similarly sheathed by edge-bridging and exo-bound iodine atoms (yellow).^{36,37} (Iodine atoms that bridge side edges on this chain connect other chains into sheets as I^{-1} while metal vertices shown empty at the top and bottom are actually bonded I^{a-1} to other chains above and below.) The same structure type is also known for $\text{Y}_4\text{I}_5\text{C}$,³⁸ but, interestingly, the above ruthenide shows appreciably compressed Pr–Ru bonds normal to the chain through the influence of $d\pi$ – $d\pi$ bonding between two metals.

Related motifs are found in $\text{Sc}_5\text{Cl}_8\text{C}$ ³⁹ as well as in $\text{Sc}_7\text{Cl}_{10}\text{C}_2$,⁶ $\text{Y}_6\text{I}_7\text{C}$,³⁸ and $\text{Pr}_3\text{I}_3\text{Ru}$ ⁴⁰ in which pairs of the same chain type are further condensed side by side, and in cubic $\text{Pr}_3\text{I}_3\text{Ir}$ ⁴¹ (and others) in which a three-dimensional condensation occurs via three nonadjacent edges of each cluster. The discovery of chains built from confacial *square antiprismatic* clusters in R_4OsBr_4 , $\text{R} = \text{Y}, \text{Er}$,⁴² is a near singularity (so far); relative atom sizes seem to be determinant. There is also the remarkable LaI , evidently not a hydride, in a 3-D NiAs-type structure in which a sizable variation from the customary c/a ratio appears to reflect enhanced La–La interactions.⁴³

Comparable Telluride Systems. Chalcogenides of the same trivalent metals reduced below RCh have never been reported, and so explorations of the scandium and yttrium tellurides were undertaken for comparison. There were several expectations: half as many anion spacers as in a cluster halide would be present for the same electron count per metal atom, and this should lead to enhanced metal aggregation; likewise, the largest

anion spacer, Te, coupled with the smallest cluster metal, Sc, should enhance the independence of the metal units. These are in general correct for the scandium (and yttrium) tellurides, but the novelty of many of the results was impossible to anticipate.

Figure 5 illustrates the structure of the “simple” Sc_2Te (a d^2 metal configuration!) in projection down the short, ~ 4 Å repeat axis.⁴⁴ What are seen are infinite “blades” constructed from puckered 10-atom rings of Sc (blue) or, perhaps more familiar, infinite cocondensed chains of edge-sharing octahedra (plus some augmentation). There are also isolated zigzag chains of Sc. The Sc–Sc distances are shortest in the center of the so-called blades, and the pairwise overlap populations make this differentiation even more emphatic (distances are not always good measures of bonding interactions!). Furthermore, the zigzag chain is, in the same terms, basically nonbonded, trapped mainly by a matrix effect of Te. Likewise, the Sc–Sc overlap populations are lower around the outside of the “blades” where the metal atoms have more Te neighbors. This is a general effect.

An extreme for a binary phase is reached for the most reduced Sc_9Te_2 , Figure 6, in which 2-D sheets are built from distorted 3×3 columns.⁴⁵ Other new telluride products contain one of the late 3d metals Mn–Ni bound within scandium chains or columns, interstitials in a sense.⁴⁶ These heterometal interactions as well as those in the halide clusters described earlier appear to reflect the extra stability that Brewer⁴⁷ first associated with early–late d-element bonding. Analogues of some of these Sc structures are also found for the electron-richer Ti, Zr chalcogenides, where the association of the host metals is generally less well differentiated.

II. Chemistry in Intermetallic Phases. Interstitials Again

Mn_5Si_3 -Type Structures. Another, but very different, family of compounds between transition metals T and main-group elements M also show extensive interstitial chemistries, namely, the large group (> 175) of fairly polar T_5M_3 phases that have Mn_5Si_3 -type structures. However, these compounds are distinctly different from the preceding in that basically all are also stable without interstitials, and they are all electron-rich and inherently metallic. The latter circumstance arises because, in the chemist’s vernacular, the valence electron supply from the active T metal (groups 2–5) exceeds that necessary to fill the lower lying valence levels of the isolated M atoms, which generally come from the Al through the P families, groups 13–15. Accordingly, there are no simple electron counting rules that need to be satisfied to confer, or by which to judge, stability, but the extra electrons are available to do chemistry.

(32) Lulei, M.; Martin, J. D.; Hoistad, L. M.; Corbett, J. D. *J. Am. Chem. Soc.* **1997**, *119*, 513.

(33) Payne, M. W.; Ebihara, M.; Corbett, J. D. *Angew. Chem., Int. Ed. Engl.* **1991**, *30*, 856.

(34) Steinwand, S. J.; Corbett, J. D. *Inorg. Chem.* **1996**, *35*, 7056.

(35) Steinwand, S. J.; Corbett, J. D.; Martin, J. D. *Inorg. Chem.* **1997**, *36*, 6413.

(36) Payne, M. W.; Dorhout, P. K.; Corbett, J. D. *Inorg. Chem.* **1991**, *30*, 1467, 3112.

(37) Park, Y.; Martin, J. D.; Corbett, J. D. *J. Solid State Chem.* **1997**, *129*, 277.

(38) Kauzlarich, S. M.; Hughbanks, T.; Corbett, J. D.; Klavins, P.; Shelton, R. N. *Inorg. Chem.* **1988**, *27*, 1791.

(39) Hwu, S.-J.; Dudis, D. S.; Corbett, J. D. *Inorg. Chem.* **1987**, *26*, 469.

(40) Payne, M. W.; Dorhout, P. K.; Kim, S.-J.; Hughbanks, T. R.; Corbett, J. D. *Inorg. Chem.* **1992**, *31*, 1389.

(41) Dorhout, P. K.; Payne, M. W.; Corbett, J. D. *Inorg. Chem.* **1991**, *30*, 4960.

(42) Dorhout, P. K.; Corbett, J. D. *J. Am. Chem. Soc.* **1992**, *114*, 1697.

(43) Martin, J. D.; Corbett, J. D. *Angew. Chem., Int. Ed. Engl.* **1995**, *34*, 233.

(44) Maggard, P. A.; Corbett, J. D. *Angew. Chem., Int. Ed. Engl.* **1997**, *36*, 1974.

(45) Maggard, P. A.; Corbett, J. D. *J. Am. Chem. Soc.* **2000**, *122*, 838.

(46) Maggard, P. A.; Corbett, J. D. *Inorg. Chem.* **1999**, *38*, 1945.

(47) Brewer, L.; Wengert, P. R. *Metall. Trans.* **1973**, *4*, 83.

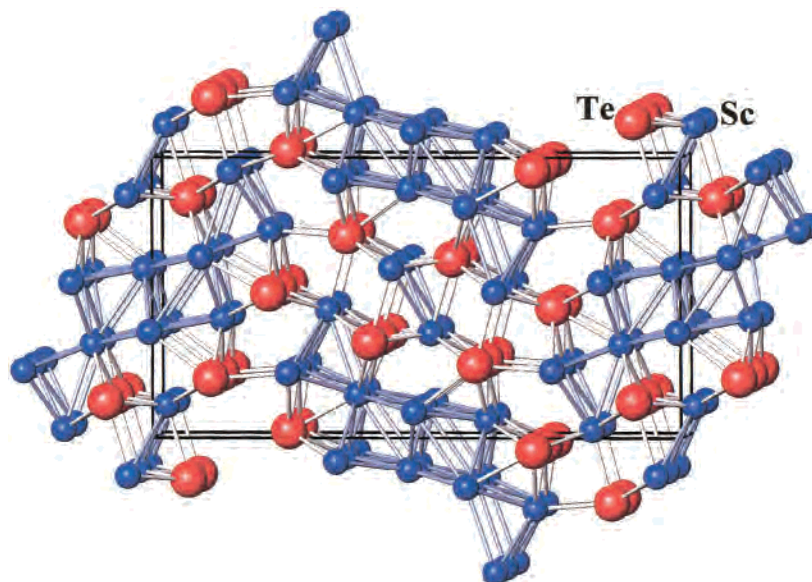


Figure 5. A section of the structure of Sc_2Te viewed down the short axis. The strongly bonded aggregates (blades) and separate chains of Sc (blue) are thus infinite in this projection.

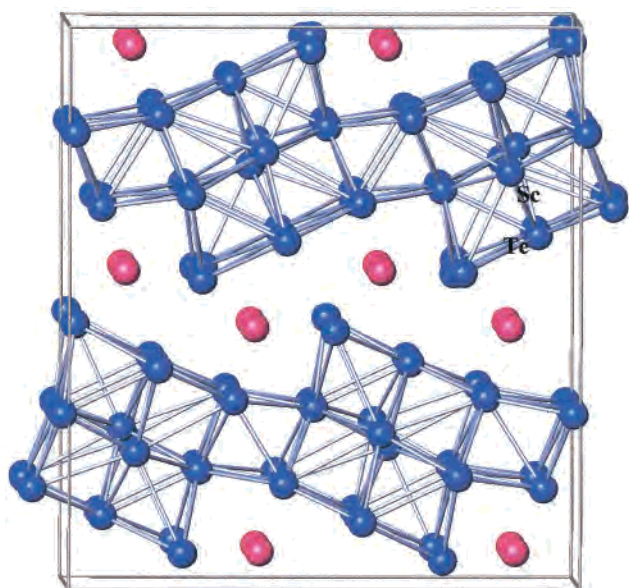


Figure 6. The more condensed structure of Sc_3Te_2 looking down infinite chains of multiply condensed (and distorted) octahedra or cubes. The strongest Sc–Sc interactions in this electron-poor compound are again in the centers of the blocks.

The ability of this structure type to take up third elements in a preformed interstitial site was first described in the 1950s by Nowotny, who at the time believed that many, if not all, phases with this structure were really ternaries, a category later named as “Nowotny phases”. This is now known to not be a common situation, although a few are indeed stable only as $\text{T}_5\text{M}_3\text{Z}$ ternaries. For the novice or the uninformed, the Mn_5Si_3 -type compounds are indeed synthetic traps, willing and able to take up a large variety of common (or other) impurities in basically the same structure with only small changes in lattice parameters and, perhaps, in intensities to announce the event, unless of course a structural refinement is performed or some element-specific analysis is pursued for a *single-phase* sample.

The essence of this remarkable hexagonal Mn_5Si_3 -type structure is shown in Figure 7 for $\text{La}_5\text{Sb}_3\text{Br}$.⁴⁸ The transition-metal component (dark blue) plays two roles, on the left as a chain of confacial antiprisms of the T metal (La2) (outlined in

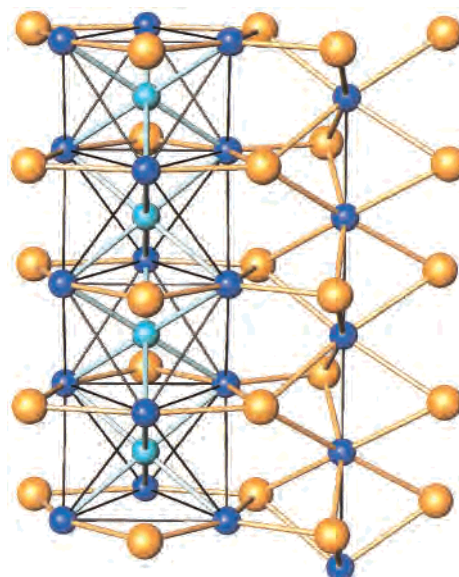


Figure 7. A [110] section of a hexagonal $\text{Mn}_5\text{Si}_3\text{Z}$ -type “stuffed” structure, here $\text{La}_5\text{Sb}_3\text{Br}$. Confacial trigonal antiprisms of La2 (dark blue atoms, outlined in black) define the “octahedral” cavities that bind a diversity of interstitial atoms (here Br, light blue). The second, linear La1 “spine” on the right is not a major factor in the chemistry. The metal units are interconnected by isolated Sb atoms (orange). Substantially all of the empty and stuffed examples are characteristically metallic.

black) and in a single string (La1) on the right. The interstitial chemistry is associated with the cavities within the former. The two metal portions are interconnected by single atoms of the main-group element (Sb) that bridge shared edges in the antiprismatic chain; these are generally presumed to be closed shell (Sb^{-3} here) in combination with the active metals. The flexibility of the structure with these preformed cavities as well as the general electronics allows binding of a diverse variety of interstitials, the lattice in effect breathing to accommodate wide ranges of radii. At one extreme, some of the excess electrons of the host fill the valence shells of the more electronegative

(48) Jensen, E. A.; Hoistad, L. M.; Corbett, J. D. *J. Solid State Chem.* **1999**, *144*, 175.

added Z, while earlier and more metallic Z appear to become involved in the metallic bonding of the host and do not open a gap.

A few special combinations of host and Z have just the right balance for the interstitial to accommodate all of the extra electrons in the parent. Examples are $\text{La}_5\text{Ge}_3\text{P}$ ($5 \times 3 - 3 \times 4 - 3$)⁴⁹ and $\text{Ca}_5\text{Sb}_3\text{Cl}$,⁵⁰ both semiconductors (and Zintl phases), but it is quite infrequent that such a situation can be created. (In addition, extreme charge transfer does not occur in the seemingly closed shell Y_5Ga_3 , etc.⁵¹) One more chemical regularity worth noting is that systems in which a stoichiometric amount of Z would require more electrons than available from the host do not form, or can be found transformed into another structure type that contains dimers (or other) of the main-group M (or Z), for instance, in La_5Ge_4 .⁴⁹ (In other words, compounds with holes in the valence band do not appear to be stable.) In general, nearly all of the ternaries have excess valence electrons and remain metallic. These characteristics thus present really new and different sorts of materials to investigate.

Typical reactions of the elements or other precursors are run in Ta at 600–1400 °C, depending mostly on the properties of the host. Most ternary products are stoichiometric and can be obtained quantitatively after suitable annealing. Guinier X-ray powder diffraction patterns are well suited to follow these reactions since the same basic pattern for T_5M_3 and $\text{T}_5\text{M}_3\text{Z}$ is seen before and after successful reactions, only a lattice constant shift and, perhaps, subtle intensity changes appearing. On the other hand, an unshifted pattern and sometimes pure Z, but more often a TZ_x product, is found when $\text{T}_5\text{M}_3\text{Z}$ is not stable. Solid solutions $\text{T}_5\text{M}_3\text{Z}_x$, $x < 1$, have been found only occasionally, although this aspect has not been widely explored. Mixed interstitials are of course possible, but presumably with boundaries or other problems when their sizes are very different.

Extensive studies of the range of possible Z have been undertaken for the hosts Zr_5Sb_3 ,⁵² Zr_5Sn_3 ,⁵³ Zr_5Pb_3 ,⁵⁴ La_5Ge_3 ,⁴⁹ La_5Pb_3 ,⁵⁵ and $(\text{M}^{\text{II}})_5(\text{Sb},\text{Bi})_3$.⁵⁰ An overview of the results in two systems, $\text{La}_5\text{Ge}_3\text{Z}$ and $\text{Zr}_5\text{Sb}_3\text{Z}$, is conveniently represented in Figure 8 in terms of cell volume vs the group of Z, with data for Z in the same period interconnected. The dashed line in each represents the volume of the empty host. Missing elements at the boundaries generally mean no $\text{T}_5\text{M}_3\text{Z}$ was formed, although some Z were not investigated in the Zr_5Sb_3 case (B, N, etc.). It is not particularly surprising that numerous lattice constants reported in the literature for Mn_5Si_3 -type binary phases indicate that significant amounts of impurity elements were in fact incorporated.

The existence of large families of these ternary products obviously affords opportunities to tune physical or chemical properties of a given host through variation of Z. One spectacular result has been a 10^4 reduction in the corrosion rate of Ti_5Si_3 in air at 1000 °C through the introduction of interstitial carbon.⁵⁶ This is thought to function by greatly reducing the diffusion rate of the surrounding titanium through constriction of and increased binding in the Ti_6C centers.

Hydride Impurities. Hydrogen may play a special (and insidious) role in solid state chemistry because it is so pervasive, not seen by the usual X-ray diffraction, and often not considered.

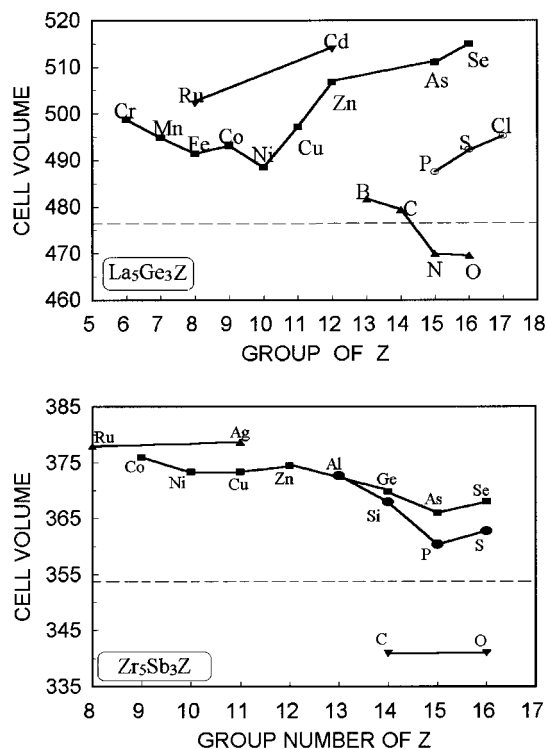


Figure 8. The range of interstitial elements Z that may be bound in $\text{Zr}_5\text{Sb}_3\text{Z}$ (bottom) and $\text{La}_5\text{Ge}_3\text{Z}$ (top). The results are presented in terms of unit cell volume vs the group of Z, with Z in the same period interconnected. The dashed line is the volume of the empty binary. Note the flexibility of the structure and the contractions afforded by the smaller Z.

We have found that hydrogen is an especially frequent impurity in commercial samples of the alkaline-earth metals, but less than careful handling can also lead to contamination of many other active metals and their compounds. Up to 5–20 atom % H in the former was fairly common in the past, but recent products are better, although not clean. The problems generally arise because these (and other) metals retain the hydrogen produced during reactions with water vapor.

Symptoms of hydrogen stabilization, as with other adventitious elements, are usually (a) a low and erratic yield, even when the reaction is loaded at the supposed stoichiometry, (b) lack of adherence to the phase rule when polytypes appear to be involved, and (c) erratic lattice constants from unrecognized variations in the impurity content. A convenient and quick diagnosis for hydrogen is often possible: whether the same material is obtained when the synthesis reaction is run under dynamic vacuum at temperatures at which the hydride components will dissociate, 600–800 °C for the alkaline-earth metals. Of course, other components of the compound could also be lost under these conditions in an open system, but this possibility is easily avoided by sealing the reaction system in a Ta or Nb container. These are nicely permeable to hydrogen above 500–600 °C, depending on one's time requirements, and 900–1000 °C will accomplish the same process quite rapidly, after which the condensed components within the container can be reacted at a suitable synthesis temperature. This route is usually quicker and more convenient than cleaning the metals ahead of time. Solid Ca–Ba begin to lose H_2 appreciably just before the metals themselves begin to sublime.

Evidently nearly *all* compounds of divalent metals reported in two particular structure types have serious, even fatal, errors because of hydrogen, the so-called β - Yb_5Sb_3 and Cr_5B_3 structure

(49) Guloy, A. M.; Corbett, J. D. *Inorg. Chem.* **1993**, *32*, 3532.

(50) Hurng, W.-M.; Corbett, J. D. *Chem. Mater.* **1989**, *1*, 311.

(51) Zhao, J.-T.; Corbett, J. D. *J. Alloys Compd.* **1994**, *210*, 1.

(52) Garcia, E.; Corbett, J. D. *Inorg. Chem.* **1990**, *29*, 3274.

(53) Kwon, Y.-U.; Corbett, J. D. *Chem. Mater.* **1992**, *4*, 1349.

(54) Kwon, Y.-U.; Corbett, J. D. *J. Alloys Compd.* **1993**, *190*, 219.

(55) Guloy, A. M.; Corbett, J. D. *J. Solid State Chem.* **1994**, *109*, 352.

(56) Williams, J. J.; Akinc, M. *Oxidation of Metals*, submitted.

types. The complex β -Yb₅Sb₃ structure was once attributed to a second modification of an Mn₅Si₃-type phase (α), but in practice the proportions of the two phases were impossible to control with sensible variables.⁵⁰ In fact, all eight reported examples of this structure are hydrides with the composition (M^{II})₅(Pn)₃H_x (Pn = pnictogen Sb, Bi).^{57,58} All also occur as binary Mn₅Si₃-type phases, most of which take up some H as a typical Z component as well (see above). At some intermediate level of hydrogen activity, nine of these (Ca, Sr, Eu, and Yb with Sb or Bi, plus the new Sm₅Bi₃H_x) transform to the ternary “ β -Yb₅Sb₃” structure, which type should now be identified as that of the earlier recognized Ca₅Sb₃F type.⁵⁰ (Fluoride can be an excellent stand-in for hydride and is easily located by routine X-ray crystallography.) These “ β ” hydride products also exhibit variable concentrations of hydrogen. It is of some novelty that EHMO band calculations utilizing the structural parameters of the reported “binary Ca₅Bi₃” clearly reveal the effects of the unseen hydrogen by the appearance of an excess of bonding calcium states in a half-filled band at E_F, which reappear in a lower H⁻ band when hydrogen is added to the calculation.

A useful requirement, that reproducible high-yield syntheses of these so-called β -polytypes be achieved, probably would have prevented most of the composition–structural errors. In fact, the extent of formation of stable hydride impurity phases with either structure type during all earlier studies of these systems had another serious consequence: the contaminations quite obscured that binary phases of a new Ca₁₆Sb₁₁ type, which we first reported as late as 1997,⁵⁹ occur in 13 out of 15 of the possible M^{II}–Pn binary systems (excluding d elements) for Pn = As, Sb, or Bi.

A second wider-spread and supposed binary structure type, Cr₅B₃, also contains a substantial family in which all reported examples were actually ternary hydrides.⁶⁰ Many of the same dipositive cations commonly (or supposedly) form binary compounds with this structure type when combined with members of the Si (tetrel) family, namely, with the structural components (A⁺²)₅(Tt₂⁻⁶)(Tt⁻⁴) in which Tt₂⁻⁶ is isoelectronic with the following halogen molecule and Tt = Si–Pb. This formulation at its simplest also suggests that the phases are closed-shell semiconductors (Zintl phases; see part III) in which the anions should be inert to oxidation unless they undergo further polymerization along with a change in structure type. None of these simple expectations is in fact correct, which illustrates again how some of our simpler chemical assessments may be lacking. Many compositions of this type react with H, D, or F sources to yield ternary derivatives with these Z anions bound in preformed tetrahedral cavities bounded by A²⁺. This result is illustrated in Figure 9 for Ca₅Sn₃Z according to the results of the X-ray and neutron diffraction studies for Z = F and D, respectively.⁶⁰ The red circles represent tin monomers and dimers, the orange circles are Ca²⁺, and the shaded green tetrahedra enclose F⁻ or D⁻ (H⁻). (We earlier discovered that these same interstitial sites would bind anions in the nominally isotopic La₅Pb₃(O,N).⁶¹)

The striking result is that most of 23 reports in the literature for this family were evidently for hydrides. In fact, *five* examples are Nowotny phases in the sense that they exist only as ternary

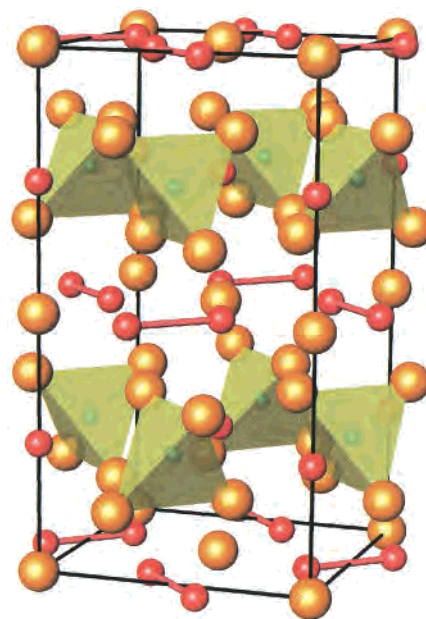


Figure 9. The stuffed tetragonal Cr₅B₃-type structure of Ca₅(Sn)₂(Sn)Z (Ca orange, Sn red) according to X-ray (Z = F) and neutron (Z = D) diffraction studies. The Z⁻ anions are centered in the shaded tetrahedra (green) defined by four Ca²⁺. Substantially all reports of (A^{II})₅Tt₃ binary phases (Tt = Si–Pb) have been in error because of unrecognized hydrogen impurities.

hydrides (and some, also as fluorides), the true binary compositions either having a different structure (e.g., W₅Si₃) or being nonexistent. This group encompasses stuffed Cr₅B₃H types in the Sr–Pb, Ba–Sn, Ba–Pb, and Yb–Sn systems, plus the more electron deficient Sr–Tl, and new members for Ca–Sn and Eu–Sn. Nine more examples in a second group, Ca–Si, Ca–Ge, Sr–Si, Sr–Ge, Sr–Sn, Ba–Si, Ba–Ge, Eu–Si, and Eu–Ge, have often been unknowingly reported for the hydrides, but the true binaries also exist with characteristically larger lattice dimensions.

These results for supposedly closed-shell binary salts raise an important question: how can one oxidize a closed-shell dimer like a halogen and retain that dimer? These particular cases appear to entail the loss of an antibonding π^* electron from Tt₂⁻⁶ in the dense solid. Indeed, the Tt–Tt bonds in the second group of compounds above often appear to shorten on formation of the hydride or fluoride. The last effect is naturally an extreme in Sr₅Tl₃H, whatever approximate charges on the anions may pertain. Some of our electron counting schemes may be too extreme or traditional, ignoring important solid state characteristics. Thus, Ca₅Ge₃ is itself metallic, suggesting that the highest lying π^* electrons are in some degree screened and delocalized at room temperature in the pure compound.⁶⁰ Again, the presence of some of the foregoing very stable hydrides during earlier studies apparently completely obscured the existence of compounds with novel combinations of tin oligomers in binary systems in which truly binary Cr₅B₃-like examples do not exist, namely, for Ca₃₁Sn₂₀, Sr₃₁Pb₂₀, Yb₃₁Pb₂₀,⁶² and Yb₃₆Sn₂₃.⁶³ Other hydride omissions have been found for what are reformulated as Ba₅Ga₆H₂⁶⁴ and Ba₂₁Ge₂O₅H₂₄.⁶⁵

(57) Leon-Escamilla, E. A.; Corbett, J. D. *J. Alloys Compd.* **1994**, 206, L15.

(58) Leon-Escamilla, E. A.; Corbett, J. D. *J. Alloys Compd.* **1998**, 265, 104.

(59) Leon-Escamilla, E. A.; Hurng, W.-M.; Peterson, E. S.; Corbett, J. D. *Inorg. Chem.* **1997**, 36, 703.

(60) Leon-Escamilla, E. A.; Corbett, J. D. *Inorg. Chem.*, submitted.

(61) Guloy, A. M.; Corbett, J. D. *Z. Anorg. Allg. Chem.* **1992**, 616, 61.

(62) Ganguli, A. K.; Guloy, A. M.; Leon-Escamilla, E. A.; Corbett, J. D. *Inorg. Chem.* **1993**, 32, 4349.

(63) Leon-Escamilla, E. A.; Corbett, J. D. *Inorg. Chem.* **1999**, 38, 738.

(64) Henning, R. W.; Leon-Escamilla, E. A.; Zhao, J.-T.; Corbett, J. D. *Inorg. Chem.* **1997**, 36, 1282.

(65) Huang, B.; Corbett, J. D. *Inorg. Chem.* **1998**, 37, 1892.

III. Polyanions of the Early p-Element Metals

A small group of very novel polyanions of Sn, Pb, Sb, and Bi has long been known following their initial characterizations in $\text{NH}_3(\text{l})$.⁶⁶ These later became known as “Zintl ions”. However, their exact constitution remained uncertain until about two decades ago when many were finally isolated from molecular solvents and structurally characterized as their alkali-metal-cryptand (or other) salts (reviews^{67,68}). An especially noteworthy feature of these results was that their cluster configurations, charges, and electronic structures meshed very well with fairly direct modifications of Wade’s rules, empirical electronic classifications of the electron-deficient (relative to octet rules) boranes(2⁻) ($\text{B}_n\text{H}_n^{2-}$) and other species. Accordingly, $2n + 2$ skeletal-based (p) electrons were deemed necessary to achieve closed-shell configurations for n -vertex closed (*closo*) delta-hedra, $2n + 4 e^-$ after one vertex was removed from the *closo* parent and n vertices remained (*nido*), $2n + 6 e^-$ with two missing vertices (*arachno*), and so forth. Some classical “naked cluster” examples for the tetrals are Sn_5^{2-} , Pb_5^{2-} (D_{3h}), Sn_9^{4-} , Ge_9^{4-} (C_{4v}), Ge_9^{2-} ($\sim D_{3h}$), TlSn_9^{3-} (D_{4d} neglecting the heteroatom), and a rare radical Sn_9^{3-} ($\sim D_{3h}$).⁶⁸ Although all of these were originally isolated from reactions in molecular solvents, several have more recently been shown to exist in “neat” solids with alkali-metal cations (review³).

A “Zintl boundary” between the Si (Tl) and the Al (Tr) families was postulated in the late 1930s to be the left border among the main-group elements for stable cluster anions. The triels were thus specifically excluded on the bases that none of their compounds with alkali metals could be obtained in liquid NH_3 , and the solid phases they formed with magnesium appeared to have intermetallic structures and properties instead. These differences are to the first degree still true; all known triel polyanions exist only in neat solid phases with the alkali metals. But more contemporary techniques have allowed researchers to characterize even a few salts of classical (Wade’s rule) triel clusters, the tetrahedral *nido*- In_4^{8-} ⁶⁹ and Tl_4^{8-} ^{70,71} as the sodium (or more complex) salts, the trigonal bipyramidal (D_{3h}) *closo*- Tl_5^{7-} in several ternary or higher phases,^{71,72} the *nido* (C_{4v}) pyramidal In_5^{9-} in La_3In_5 ,⁷³ and octahedral Ga_6^{8-} in $\text{Ba}_5\text{Ga}_6\text{H}_2$ ⁶⁴ and Tl_6^{8-} in some more complex quaternary phases (below). (Note that all of these superscripts are intended to denote oxidation state sums, not real charges, and they were arrived at according to only the structure and stoichiometry.) These trielides of more or less traditional clusters necessarily have higher charges than for later elements (the ideal *closo* species are Tl_n^{-2} vs Tr_n^{-2-n}), and this is quite consistent with the appearance of the trielides only as salts in the compact solid state, as opposed to their synthesis via molecular solvents. In other words, the Madelung energy of the neat salts is clearly greater than acid–base, ion–dipole, etc. interactions that pertain to solutions.

A second distinctive feature of the majority of triel polyanions is that they are *hypo-electronic*, that is, short of cluster-based electrons relative to Wade’s correlations. This seems a fairly natural happenstance, but it is new largely because the minimum electronic requirements and the stability of such species had

Table 2. Beyond the Zintl Border. I. Hypoelectronic Homoatomic Clusters of Triel Elements

| ion | compound | cluster symmetry | skeletal p electrons, ^a count | | ref |
|-----------------------|------------------------------------------------------------------------|------------------|------------------------------------------|----------|---------|
| | | | | | |
| Tl_6^{6-} | KTl | $\sim D_{2h}$ | 12 | $2n$ | 75 |
| | CsTl | $\sim D_{4h}$ | | | 76 |
| Tl_7^{7-} | $\text{Na}_{12}\text{K}_{38}\text{Tl}_{48}\text{Au}_2$ | $\sim D_{5h}$ | 14 | $2n$ | 77 |
| | $\text{K}_{10}\text{Tl}_7^b$ | | | | 78 |
| Tl_9^{9-} | $\text{Na}_2\text{K}_{21}\text{Tl}_{19}$ | C_{2v} | 18 | $2n$ | 72 |
| | $\text{Na}_{12}\text{K}_{38}\text{Tl}_{48}\text{Au}_2$ | C_{2v} | | | 77 |
| Ga_{11}^{7-} | $\text{Cs}_8\text{Ga}_{11}^b$, $\text{Cs}_8\text{Ga}_{11}\text{Cl}^c$ | $\sim D_{3h}$ | 18 | $2n - 4$ | 79 |
| In_{11}^{7-} | $\text{K}_8\text{In}_{11}^b$ | $\sim D_{3h}$ | 18 | $2n - 4$ | 80 (79) |
| Tl_{11}^{7-} | $\text{A}_8\text{Tl}_{11}^b$, $\text{A} = \text{K}-\text{Cs}$ | $\sim D_{3h}$ | 18 | $2n - 4$ | 81 |
| | $\text{A}_{15}\text{Tl}_{27}^b$, $\text{A} = \text{Rb}, \text{Cs}$ | D_{3h} | | | 82 |
| | $\text{K}_{18}\text{Tl}_{20}\text{Au}_3^b$ | D_{3h} | | | 83 |

^a Skeletal electron counts exclude ns^2 cores. ^b Metallic phase with excess electrons; stoichiometric but not electron precise. ^c Other $\text{A}_8\text{Tr}_{11}\text{X}$ examples were also identified.

simply never been tested before. The surprises also extend to new clusters that are centered by either the same atom or a heteroatom. Finally, novel and unprecedented extended structures are also found for both Tr and Tt families, taking us into the broader arena of Zintl (valence) compounds.⁷⁴ There are also some worthwhile general considerations: why are the metal–metal bonding characteristics of these elements so pronounced, and why as anions? The latter must arise because the species are basically very electron-deficient. And as we progress further to the left in the main-group metals, where and how do their compounds with the active metals eventually begin to act as intermetallic phases as opposed to salts? Those answers are yet to come. And can we have Zintl phase salts that are intrinsically metallic in spite of evident closed electron counts, or others that have well-recognized clusters in the presence of excess electrons (metallic salts). The evidence says yes to both.

Beyond the Zintl Boundary. Hypoelectronic Clusters. Table 2 lists the uncentered homoatomic triel clusters that we have found to achieve closed-shell bonding with $2n$ or fewer electrons. (Aluminum is excluded hereafter; although it shows some remarkable chemistry, none of it (except for LiAl) shows any similarity to that of Ga, In, Tl.) The first two in the Table, Tl_6^{6-} and Tl_7^{7-} , reach this status by a familiar Jahn–Teller-type process, axial compression of the classical *closo*- ($2n + 2$) Tl_6^{8-} and the hypothetical Tl_7^{9-} . Only the last achieves a formal transannular bond, as shown at the top in Figure 10. The three Tr_{11}^{7-} species listed are among the most novel of the new clusters because of the unfamiliar geometry, upper right in Figure 10. This can be formally derived from a conventional tricapped trigonal prism Tr_9^{11-} ($2n + 2 e^-$, D_{3h}) through the addition of two axial Tr^+ (s^2) ions along the 3-fold axis to give a pentacapped intermediate Tr_{11}^{9-} . The direct product is not very plausible since it is neither very spherical nor uniformly bonded, but an axial compression and lateral expansion that opens up the basal faces of the original prism (and eliminates the formerly π bonding MO therein) gives the observed

(66) Zintl, E.; Goubeau, J.; Dullenkopf, W. *Z. Phys. Chem., Abt. A* **1931**, *154*, 1.

(67) Corbett, J. D. *Chem. Rev.* **1985**, *85*, 383.

(68) Corbett, J. D. *Struct. Bonding* **1997**, *87*, 157.

(69) Sevov, S. C.; Corbett, J. D. *J. Solid State Chem.* **1993**, *103*, 114.

(70) Smith, J. F.; Hansen, D. A. *Acta Crystallogr.* **1967**, *22*, 836.

(71) Dong, Z.-C.; Corbett, J. D. *Inorg. Chem.* **1996**, *35*, 3107.

(72) Dong, Z.-C.; Corbett, J. D. *J. Am. Chem. Soc.* **1994**, *116*, 3429.

(73) Zhao, J.-T.; Corbett, J. D. *Inorg. Chem.* **1995**, *34*, 378.

(74) Corbett, J. D. In *Chemistry, Structure and Bonding of Zintl Phases and Ions*; Kauzlarich, S., Ed.; VCH Publishers: New York, 1996; Chapter 3, p 139.

(75) Dong, Z.-C.; Corbett, J. D. *J. Am. Chem. Soc.* **1993**, *115*, 11299.

(76) Dong, Z.-C.; Corbett, J. D. *Inorg. Chem.* **1996**, *35*, 2301.

(77) Huang, D. P.; Dong, Z.-C.; Corbett, J. D. *Inorg. Chem.* **1998**, *37*, 5881.

(78) Kaskel, S.; Corbett, J. D. *Inorg. Chem.* **2000**, *39*, 778.

(79) Henning, R. W.; Corbett, J. D. *Inorg. Chem.* **1997**, *36*, 6045.

(80) Sevov, S. C.; Corbett, J. D. *Inorg. Chem.* **1991**, *30*, 4875.

(81) Dong, Z.-C.; Corbett, J. D. *J. Cluster Sci.* **1995**, *6*, 187.

(82) Dong, Z.-C.; Corbett, J. D. *Inorg. Chem.* **1996**, *35*, 1444.

(83) Dong, Z.-C.; Corbett, J. D. *Inorg. Chem.* **1995**, *34*, 5042.

Table 3. Beyond the Zintl Border. II. Hypoelectronic Clusters of Triel Elements

| ion | compound | cluster symmetry | skeletal p electrons, count ^a | | ref |
|----------------------------------------------------------------------|---------------------------------------------------------------------------------|-----------------------------------------------|------------------------------------------|----------------|-----|
| | | | | | |
| substituted | | | | | |
| Tl ₉ Au ₂ ⁹⁻ | K ₁₈ Tl ₂₀ Au ₃ ^b | <i>D</i> _{3h} | 16 | 2 <i>n</i> - 6 | 83 |
| Tl ₈ Cd ₃ ¹⁰⁻ | Na ₉ K ₁₆ Tl ₁₈ Cd ₃ ^c | <i>D</i> _{3h} | 18 | 2 <i>n</i> - 4 | 84 |
| In ₁₀ Hg ⁸⁻ | K ₈ In ₁₀ Hg | ~ <i>D</i> _{3h} | 18 | 2 <i>n</i> - 4 | 85 |
| centered | | | | | |
| In ₁₀ Zn ⁸⁻ | K ₈ In ₁₀ Zn | <i>D</i> _{4d} | 20 | 2 <i>n</i> | 86 |
| Tl ₁₀ Zn ⁸⁻ | K ₈ Tl ₁₀ Zn | <i>D</i> _{4d} | | | 87 |
| Ga ₁₀ Ni ¹⁰⁻ | Na ₁₀ Ga ₁₀ Ni | ~ <i>C</i> _{3v} | 20 | 2 <i>n</i> | 88 |
| In ₁₀ M ¹⁰⁻ | { K ₁₀ Tr ₁₀ M, M = Ni, Pd, Pt | ~ <i>C</i> _{3v} | 20 | 2 <i>n</i> | 89 |
| Tl ₁₀ M ¹⁰⁻ | | | | | |
| Tl ₁₁ Pd ⁷⁻ | A ₈ Tl ₁₁ Pd, A = K, Cs | ~ <i>D</i> _{3h} | 18 | 2 <i>n</i> - 4 | 90 |
| Tl ₁₃ ¹⁰⁻ | Na ₄ A ₆ Tl ₁₃ , ^c A = K, Rb, Cs | <i>T</i> _h | 25 | 2 <i>n</i> + 1 | 91 |
| Tl ₁₃ ¹¹⁻ | Na ₃ K ₈ Tl ₁₃ | <i>D</i> _{3d} | 26 | 2 <i>n</i> + 2 | 91 |
| Tl ₁₂ Na ¹³⁻ , Tl ₆ H ⁷⁻ | Na ₁₅ K ₆ Tl ₁₈ H | <i>T</i> _h , <i>O</i> _h | 26, 14 | 2 <i>n</i> + 2 | 92 |
| Tl ₁₂ M ¹²⁻ (Tl ₆ ⁸⁻) | Na ₁₄ K ₆ Tl ₁₈ M, M = Mg, Zn, Cd, Hg | <i>T</i> _h | 26, 14 | 2 <i>n</i> + 2 | 93 |

^a *n* value does not include centering atom. ^b Metallic phase; stoichiometric but not electron precise. ^c Curie–Weiss paramagnetic salt.

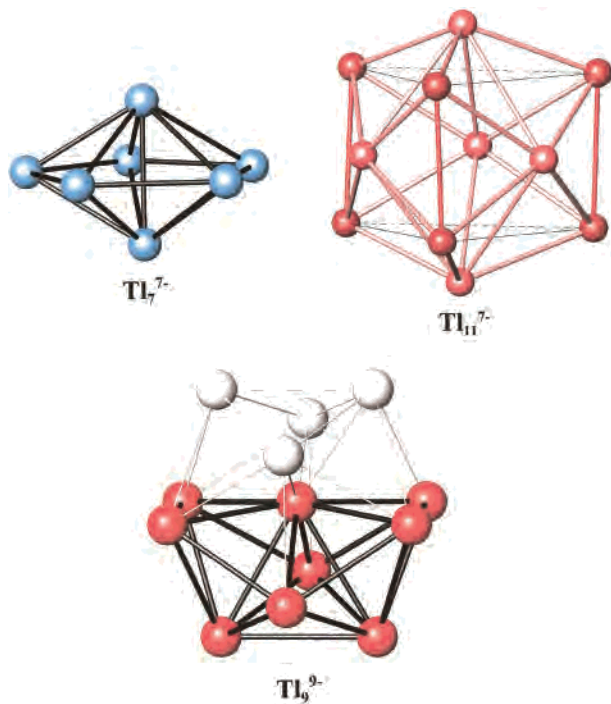


Figure 10. Three hypoelectronic clusters of thallium. Top left: Pentagonal bipyramidal Tl₇⁷⁻. Top right: The pentacapped trigonal prismatic Tl₁₁⁷⁻ (the trigonal prismatic atoms are somewhat darker). Bottom: The Tl₉⁹⁻ polyhedron (*C*_{2v}) and the four extra atoms that define its relationship to a centered icosahedron.

geometry and charge for Tr₁₁⁷⁻, 2*n* - 4 in skeletal (p) electrons. (The atoms defining the trigonal prism are shown somewhat darker.) Additional bonds or interactions between the two types of capping atoms also appear. An additional, strictly solid state phenomenon pertains to the A₈Tr₁₁ compositions containing these anions, which must be formulated as (A⁺)₈(Tr₁₁⁷⁻)e⁻ with an extra cation plus electron, evidently necessities for good packing. In other words, these are truly metallic salts with undistorted closed-shell anions (*D*₃ and close to *D*_{3h})! (A family of diamagnetic semiconductors in the same basic structure can also be obtained for many examples, e.g., Cs₈Ga₁₁Cl, Table 2.) Finally, the totally unexpected Tl₉⁹⁻ shown at the bottom of Figure 10 has a plausible parent in the forthcoming Tl₁₃¹¹⁻ anion, which is a centered icosahedron.

The fecundity of this new area is nicely emphasized by the range of substituted or centered ternary or higher triel cluster compounds that have been discovered, Table 3. All of these are seemingly unique to the three Tr elements, principally for In and Tl. Among the three substituted members, Tl₈Cd₃¹⁰⁻ and In₁₀Hg⁸⁻ are isoelectronic with Tr₁₁⁷⁻, the substitutions taking place at the waist capping atoms and randomly on the trigonal prismatic positions, respectively. The unusual Tl₉Au₂⁹⁻, Figure 11, can be derived from Tl₁₁⁷⁻ starting with axial substitution of isoelectronic Au⁻ atoms for two Tl⁺. The undistorted intermediate Tl₉Au₂¹¹⁻ is four electrons short, which is remedied by a strong axial compression to form a transannular Au–Au bond and to eliminate 2e⁻ (the out-of-phase axial p_z) from the bonding orbital set. The Au atoms basically lie in the basal planes of the thallium figure. Isolated Au⁻ ions have also been found in other salts, evidently as useful electron traps as well as “small” anions that fill sites and reduce repulsions among alkali-metal cations. (Halide probably would do likewise.)

The centered examples in the same table represent a basically new thrust in main-group-element clusters, although they harken back to a very different sort of cluster chemistry, the transition-metal halide (and other) clusters that also *require* interstitial atoms for stability (this article, part D). The binding characteristics or principles are similar. Thus, the In₁₀Zn⁸⁻ cluster (middle, Figure 11) can be imagined to derive from a classical (hypothetical) *closo*-In₁₀¹²⁻, a bicapped square antiprism, first through lateral expansion to open up edges of the square faces and to eliminate the corresponding bonding MOs. This In₁₀¹⁰⁻ intermediate now has the vertices more nearly equidistant from the Zn²⁺ that is inserted to gain the observed In₁₀Zn⁸⁻. Formally, it is the effective charge on Zn²⁺ that lowers the total skeletal count to 2*n*. (A filled a₁ cluster MO mixes with Zn 4s, and the

(84) Huang, D. P.; Corbett, J. D. *Inorg. Chem.* **1999**, *38*, 316.

(85) Sevov, S. C.; Ostenson, J. E.; Corbett, J. D. *J. Alloys Compd.* **1993**, *202*, 289.

(86) Sevov, S. C.; Corbett, J. D. *Inorg. Chem.* **1993**, *32*, 1059.

(87) Dong, Z.-C.; Henning, R. W.; Corbett, J. D. *Inorg. Chem.* **1997**, *36*, 3559.

(88) Henning, R. W.; Corbett, J. D. *Inorg. Chem.* **1999**, *38*, 3883.

(89) Sevov, S. C.; Corbett, J. D. *J. Am. Chem. Soc.* **1993**, *115*, 9089.

(90) Kaskel, S.; Corbett, J. D. To be submitted for publication.

(91) Dong, Z.-C.; Corbett, J. D. *J. Am. Chem. Soc.* **1995**, *117*, 6447.

(92) Dong, Z.-C.; Corbett, J. D. *Inorg. Chem.* **1995**, *34*, 5709.

(93) Dong, Z.-C.; Corbett, J. D. *Angew. Chem., Int. Ed. Engl.* **1996**, *35*, 1006.

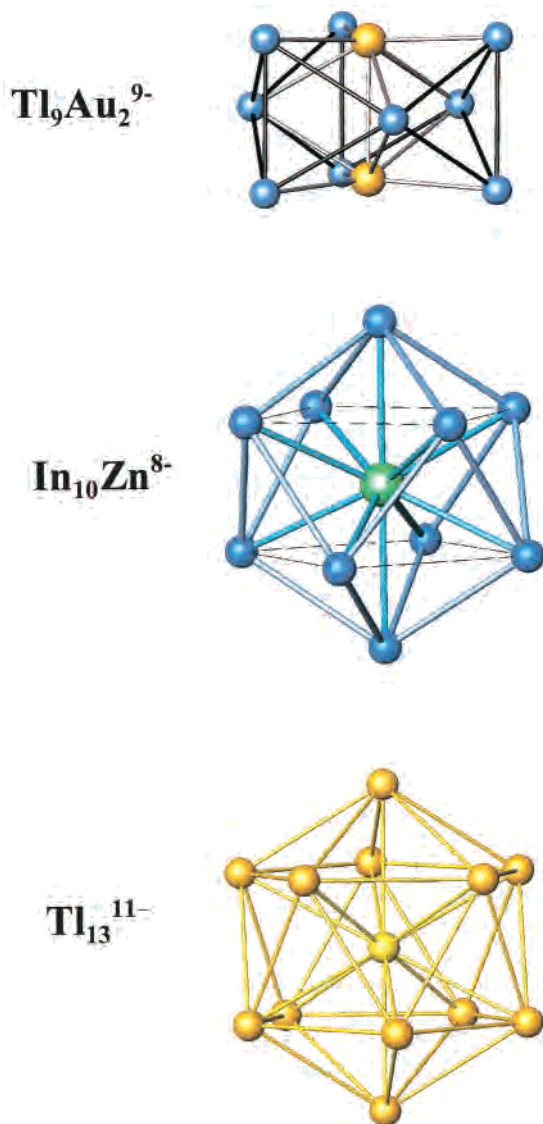


Figure 11. Three substituted or centered triel clusters: $\text{Tl}_9\text{Au}_2^{9-}$ (D_{3h}), $\text{In}_{10}\text{Zn}^{8-}$ derived from a biccapped Archimedean antiprism (D_{4d}), and the centered icosahedral Tl_{13}^{11-} (D_{3d}).

same applies for its 4p orbitals. Insertion of neutral Zn instead would result in loss of 2e from a_1^* .)

The novel $\text{Tr}_{10}\text{M}^{10-}$ species for (in part) $\text{M} = \text{Ni}, \text{Pd}, \text{Pt}$ (Table 3) differ markedly from the configuration of the isoelectronic $\text{In}_{10}\text{Zn}^{8-}$, resembling more nearly *tetracapped* trigonal prisms that retain one small basal face ($\sim C_{3v}$). This unique variation appears to result because there are two more cations to be accommodated. The cluster therefore takes on a more open character following our observations that cations are always found intimately associated with the anionic polyhedra, especially on their edges and faces (below). The Ni etc. bonding in these well-reduced clusters arises largely via its 4s and 4p orbitals (as with Zn^{2+} above), whereas the $3d^{10}$ levels lie much lower and are basically nonbonding. A remarkable new $\text{Tl}_{11}\text{Pd}^{7-}$, which is roughly isosteric and formally isoelectronic with Tl_{11}^{7-} plus an inert $4d^{10}$ core, achieves central bonding in qualitatively the same way as the foregoing $\text{Tr}_{10}\text{Ni}^{10-}$. It is the first centered example of this polyhedral type. But there are three nonequivalent types of thallium in this particular cage, and expansion of the cluster by the centering atom is not uniform, the largest occurring with the five face-capping atoms. Note that these

compounds occur in the same structure type as A_8Tl_{11} , again with one extra cation and electron.

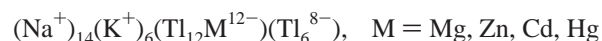
A new category of cluster arises with icosahedral $\text{Tl}_{13}^{10-},^{11-}$, the first self-centered (and egotistical?) triel clusters that are so far known only for thallium. The Tl_{13}^{11-} shown at the bottom of Figure 11 may be generated simply from a Wade's rule *closo*- Tl_{12}^{14-} by the addition of a centering Tl^{3+} (the result is no longer hypoelectronic). Salts of these icosahedral ions show very clear evidence for a strong, preferred packing of cations in specific positions about these large anions. In fact, the reader will note many other examples of new compounds in Tables 2 and 3 that are found only with mixed, but ordered, cations. This evidence of improved packing with particular combinations of cation sizes has been exploited synthetically in many parts of this work.

In the case of the line compound $\text{Na}_4\text{A}_6\text{Tl}_{13}$ ($\text{A} = \text{K}, \text{Rb}, \text{Cs}$), the packing in this body-centered-cubic cell, upper left in Figure 12, is especially effective in terms of tight sodium interbridging between clusters (along the body diagonals). As a result, the Tl_{13}^{10-} ion (point group T_h) is accommodated even though an electron hole remains in the HOMO of each cluster. (The compounds are Curie–Weiss paramagnetic.) (A novel isostructural and diamagnetic derivative has been found in $\text{Na}_2\text{Cd}_2\text{K}_6(\text{Tl}_{12}\text{Cd})$, in which Cd^{2+} is disordered over 50% of the Na^+ sites.⁹⁴) On the other hand, the closed-shell Tl_{13}^{11-} (D_{3d}) alone has been achieved only with a different but fixed cation proportion, $\text{Na}_3\text{K}_8\text{Tl}_{13}$, and in a lower symmetry rhombohedral space group (upper right, Figure 12). The specificity of cation interactions in both of these structure types is striking. There is a cation closely bound above each face and vertex of each nominal icosahedron to achieve $20 + 12 = 32$ well-packed cations in the first "solvation" sphere. This continues, and is essential for, the following derivatization of the 4–6–13 phase, but close and specific cation associations are also found about most of the other polyanion salts noted herein.⁹⁵

The cubic cell ($Im\bar{3}m$) of the former $\text{Na}_4\text{A}_6\text{Tl}_{13}$ turns out to be amenable to specific cation and anion substitutions. Conversion from the centered to the primitive cubic cell $Pm\bar{3}$ doubles the formula of the independent unit to $\text{Na}_8\text{K}_{12}(\text{Tl}_{13})_2$, and a substitution of half the K positions by Na better accommodates the forthcoming higher field octahedral cluster inserted at the body center, Figure 12 bottom. The two independent cluster sites may be occupied in several ways to give closed-shell products with heteroatoms in the icosahedra, namely, as



and



Other variations on this theme probably exist.

Networks. Many examples of *Zintl phases* are known, and these demonstrate the numerous and diverse ways in which "octet rule" bonding of p elements may be achieved in mono- and polyatomic anions and in anionic networks.⁹⁶ The variety, particularly those built from group 14 (tetrel) elements and beyond, is quite amazing. For example, the "passion" with which Sn–Sn bonding generates sometimes complex solutions to the octet rule is noteworthy.^{62,63,97,98} (A lone hyperelectronic

(94) Tillard-Charbonnel, M. M.; Belin, C. H. E.; Manteghetti, A. P.; Flot, D. M. *Inorg. Chem.* **1996**, *35*, 2583.

(95) Corbett, J. D. Unpublished.

(96) Kauzlarich, S., Ed. *Chemistry, Structure and Bonding of Zintl Phases and Ions*; VCH Publishers: New York, 1996.

(97) Zhao, J.-T.; Corbett, J. D. *Inorg. Chem.* **1994**, *33*, 5721.

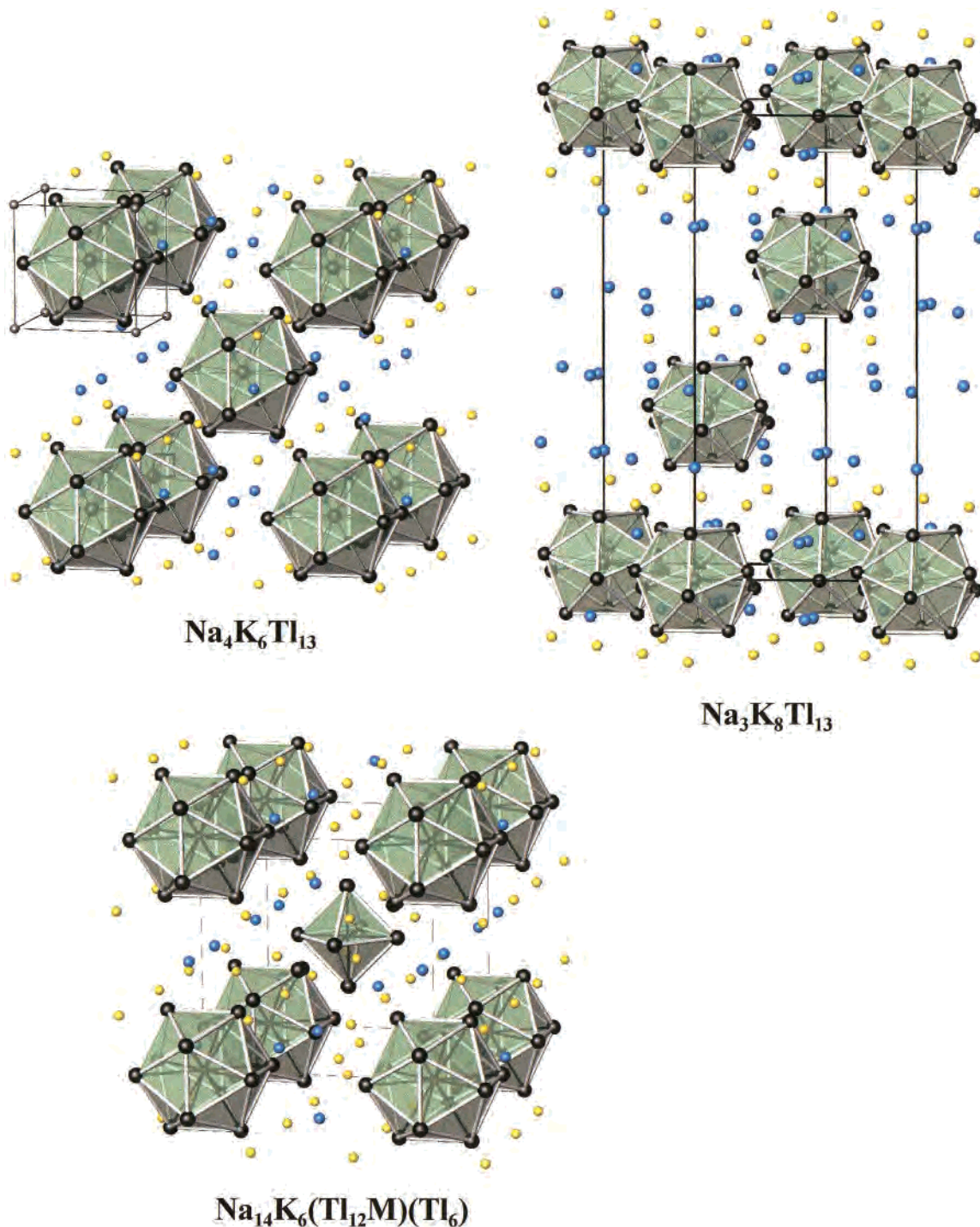


Figure 12. Unit cells of three structures that contain centered isocahedra of Tl_{13} . The sodium atoms are yellow, potassium, blue. Top left: Cubic $\text{Na}_4\text{K}_6\text{Tl}_{13}$ with T_h paramagnetic clusters Tl_{13}^{10-} . Face-centered Na atoms on the cell diagonals bridge between clusters. Top right: The rhombohedral $\text{Na}_3\text{K}_8\text{Tl}_{13}$ unit cell with D_{3d} Tl_{13}^{11-} clusters. Bottom: The primitive cubic cell of $\text{Na}_{14}\text{K}_6(\text{Tl}_{12}\text{M})(\text{Tl}_6)$ and other compositions. See the text for the relationship between the two cubic systems and the other examples. Reprinted with permission from Corbett, J. D. *Angew. Chem., Int. Ed.* **2000**, *39*, 670. Copyright 2000 Wiley-VCH.

example is also found in chains of square-planar tin in $\text{Ca}_{6.2}\text{Mg}_{3.8}\text{Sn}_7$.⁹⁹ Of course, the earlier triels would be expected to generate networks built from more delocalized, electron-deficient clusters distantly parallel to the boron hydrides, etc., and this seems to be the case without exception. Some of these structures and their bonding are quite complex, even inexplicable, especially for gallium.³ For reasons of time and space,

this presentation will limit the discussion to examples of three, the simple network of octahedra in K_2Ga_3 , Rb_2In_3 , etc., the remarkable infinite columns of condensed, Cd-centered, thallium pentagonal antiprisms in $\text{Cs}_5\text{Tl}_{11}\text{Cd}_2$, and the granddaddy of all, the In_{70} example of a multiply-shelled “fullerane” in $\text{Na}_{172}\text{In}_{197}\text{Z}_2$, $Z = \text{Ni}, \text{Pd}, \text{Pt}$.

The top of Figure 13 shows one layer of gallium octahedra in K_2Ga_3 that are interconnected via bonds between the waist atoms of each.⁸⁸ The closed-shell nature of this Zintl phase may be easily demonstrated starting with the classical octahedral

(98) Vaughney, J. T.; Corbett, J. D. *Inorg. Chem.* **1997**, *36*, 4316.

(99) Ganguli, A. K.; Corbett, J. D.; Köckerling, M. *J. Am. Chem. Soc.* **1998**, *120*, 1223.

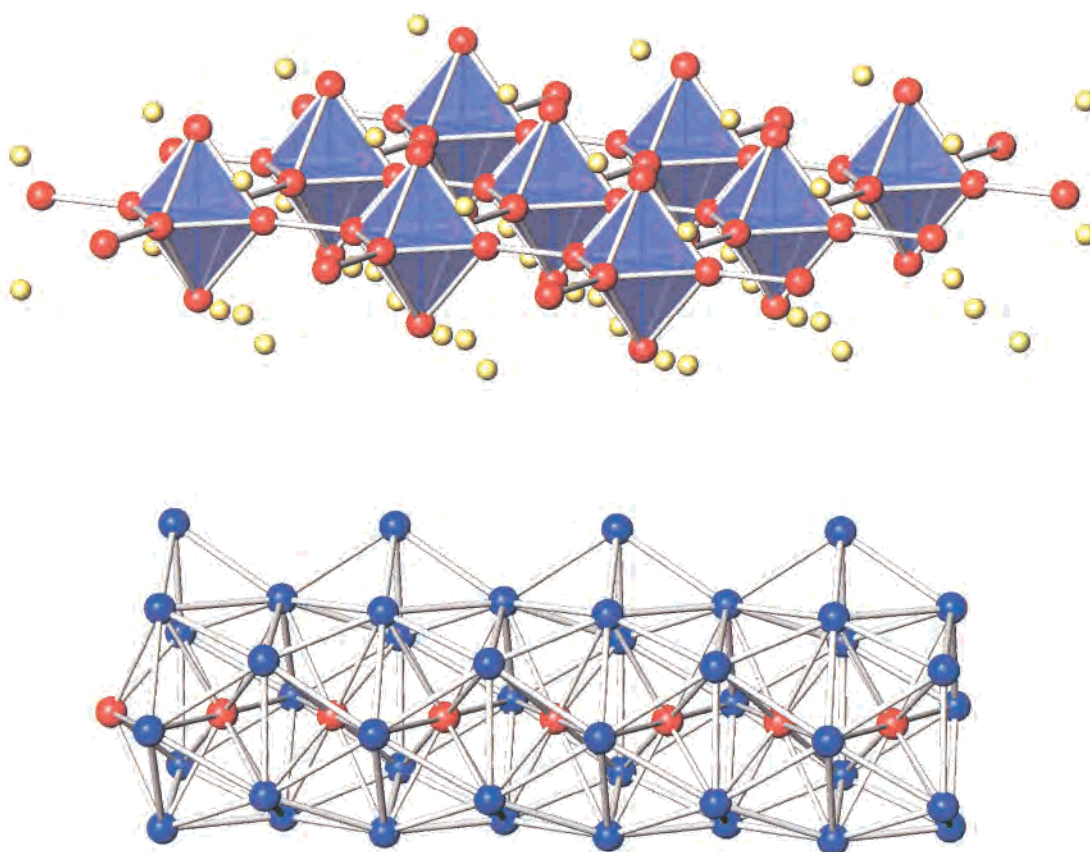


Figure 13. Top: The layer of gallium octahedra (red) in K_2Ga_3 that are interbonded at four waist vertices. Bottom: A segment of the ${}^1_{\infty}[Tl_{11}Cd_2^{5-}]$ rods in $Cs_5Tl_{11}Cd_2$ that are built from confacial Cd-centered Tl_{10} pentagonal antiprisms. Note the additional Tl atoms bonded at the top of the chain.

Ga_6^{8-} . Intercluster bonds, generally shorter than within clusters, are evidently regular $2c-2e$ types, and their formation can be viewed as originating from one-electron oxidations of the s^2 pair at each vertex. In this case, oxidation of four coplanar centers of the octahedra gives Ga_6^{4-} units, and these yield the ${}^2_{\infty}[Ga_6^{4-}]$ sheets shown when coupled. The cations lie between the layers.

Understanding the ${}^1_{\infty}[Tl_{11}Cd_2^{5-}]$ column in $Cs_5Tl_{11}Cd_2$ ¹⁰⁰ that is shown at the bottom of Figure 13 is not so easy. These consist of Tl_{10} square antiprisms that are each centered by a cadmium atom and condensed via shared basal faces into columns or rods, which stack in a 2-D close-packed pattern separated by Cs^+ ions. The condensation process can be followed theoretically starting with cyclopentadiene-like units, but the necessity of the centering atom (only Cd to date) and the additional feature of added Tl “fins” on one side of the column are harder to understand. The latter do confer acentricity to the columns. Band theory calculations suggest that the chains are metallic, consistent with the bulk properties of the powdered solid. The phase is found only with Cs or Rb, whereas the smaller K presumably favors the formation of other phases with denser cation packing about the clusters, K_8Tl_{11} and $K_{15}Tl_{27}$ for instance. The discovery is quite extraordinary and certainly unprecedented.

Exploratory syntheses in indium systems yielded many surprises, the biggest of which occurred when a sodium reactant was substituted at stoichiometries that had earlier given the potassium cluster phases $K_{10}In_{10}Z$, $Z = Ni, Pd, Pt$ (Table 3). Sodium appears unique (to date) in its capacity to serve as a

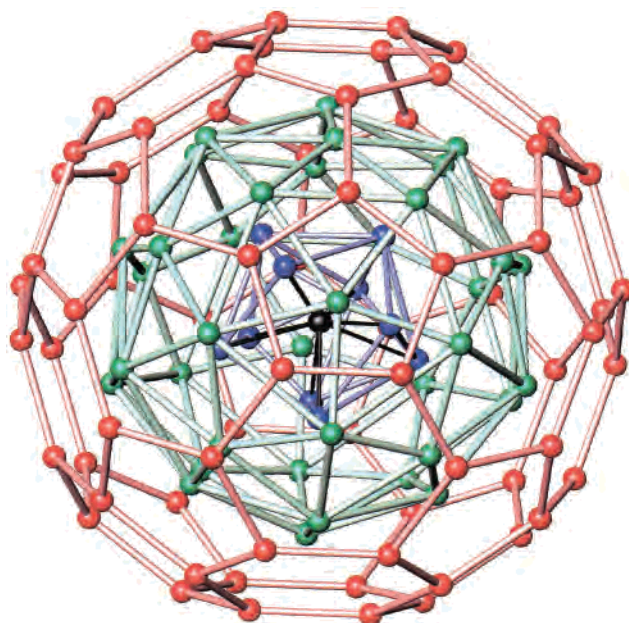


Figure 14. The multiply-endoheral $Ni@In_{10}@Ni_{37}@In_{70}$ cluster extracted from the structure of $Na_{172}In_{197}Ni_2$ with atoms in this sequence colored black, blue, green, and red, respectively. Each Na lies below the center of each pentagonal or hexagonal face of the In_{70} fullerene, but interconnections within the green Na_{37} polyhedron are meant only to guide the eye.

spacer in multiply-endoheral indium shell structures, the outer member of which classifies as a fullerene or saturated “buckyball”. Two types of structures have been characterized, hexagonal $Na_{96}In_{97}Z_2$ ¹⁰¹ and orthorhombic $Na_{\sim 172}In_{\sim 197}Z_2$,¹⁰²

with $Z = \text{Ni, Pd, Pt}$ in both. (Notice how close the first phase is to the composition NaIn , a known stuffed diamond structure, save for a very few Z!) Each compound contains several types of endohedral polyhedra or “onions”, the most interesting being $\text{Ni@In}_{10}\text{@Na}_{39}\text{@In}_{74}$ and $\text{Ni@In}_{10}\text{@Na}_{37}\text{@In}_{70}$, respectively, in which the shells are enumerated from the central Ni atom in an $\text{In}_{10}\text{Ni}^{10-}$ cluster outward. Fortunately, the last was already known, Table 3, but with only $\sim C_{3v}$ symmetry. This is incompatible with the symmetry of the present structures, and so some disorder was found because of the higher imposed crystal symmetry. That within the latter In_{70} member was simpler to resolve, and the overall result is shown in Figure 14.

In both cases, classical fullerene configurations are found for the In_{74} and In_{70} shells, which are likewise constructed of fused pentagonal and hexagonal rings, the former always being surrounded by six hexagons, and so on. Each face of the present In_{70} polyhedron (red) is capped on the inside (and also on the outside, not shown) by a sodium atom (green), which atoms then define the complimentary Na_{37} polyhedron. Note that the Na atoms are interconnected in Figure 14 only to guide the eye and certainly not to imply bonds! The Na atoms that cap pentagons in In_{70} lie somewhat more inward in the figure, and it is these that serve to restrict the possible orientations of $\text{In}_{10}\text{Ni}^{10-}$ (blue, black) in the center. But readers beware, this

pretty picture has been carved from a complex condensed solid state structure! Indium would not be expected to exhibit good π bonding, as is present in real fullerene molecules, and instead each vertex in In_{70} etc. gains a fourth outward-directed σ bond to another In (a) via condensation of these fullerene units with others through shared pentagonal faces to form puckered layers, or (b) via intercage bonds that adjoin the fusion links, or (c) through the addition of small external In rings (“warts”) elsewhere (not shown). Marvelous indeed!

This wonderful compound allows us to close with an outstanding example of the excitement and joy that may be the other products of a successful pursuit in exploratory synthesis. There are *many* wonders still to be discovered!

Acknowledgment. The first part of this article describes research supported by NSF—Solid State Chemistry, presently by Grant DMR-9809850. The second and third parts excerpt work supported by the U.S. Department of Energy, Basic Energy Sciences, Materials Sciences Division. All of the research has been carried out the Ames Laboratory, which is operated for DOE by Iowa State University under Contract W-7405-Eng-82. The accomplishments described are all attributable to the talents of an exceptional group of undergraduate, graduate, and postdoctoral co-workers whose names appear in the references. Little could have been accomplished without them.

(101) Sevov, S. C.; Corbett, J. D. *Science* **1993**, 262, 880.

(102) Sevov, S. C.; Corbett, J. D. *J. Solid State Chem.* **1996**, 123, 344.